

Letters

Integrating Sensing Coil Function into Field Winding for Initial Position Estimation of Nonsalient DC Vernier Reluctance Machine

Weiyu Wang , Shuangxia Niu , *Senior Member, IEEE*, and Xing Zhao , *Member, IEEE*

Abstract—This letter presents a novel mutual inductance detection method by integrating sensing coil function into field winding for the initial position estimation of nonsalient DC-excited vernier reluctance machines (DC-VRM). The key is to reutilize the field winding as a sensing coil by operating the power transistor states, and then the induced currents can be detected from the closed sensing coil when detection pulses are injected into the armature windings. Combined with the established mutual inductance model, reliable position estimation is easily achieved without additional detection circuits. The proposed method has good potential to be applied to a group of nonsalient machines with independent field and armature windings.

Index Terms—DC-excited Vernier reluctance machine (DC-VRM), initial position estimation, sensorless drive.

I. INTRODUCTION

A. Research Motivations

With an increasing concern for environmental protection and energy saving, research on transportation electrification has attracted more attention [1]. Electrical machines are exposed to new challenges of harsh environmental adaption, cost-saving, and reliability. Developing no-permanent magnet reluctance machines has been a hot research topic. Switched reluctance machine (SRM) suffers from large torque ripple and noises [2]. The doubly fed doubly salient machine (DF-DSM) has an unbalanced magnetic distribution [3]. Compared with these counterparts, dc-excited Vernier reluctance machine (DC-VRM), has small torque ripples and cogging torque [4] and has good potential to be applied as an integrated starter and generator (ISG).

Position sensorless drives can save costs and further guarantee system reliability [5], [6], [7], [8], [9], [10], [11], [12], [13], [14],

[15], [16], [17], [18], [19]. By exciting windings with preset commutation logic signals, the open loop method [5] can start up the machine without rotor initial position information, while the startup jitter and reverse cannot be avoided, which should be forbidden in safety-critical applications. Therefore, initial position estimation becomes an important step to starting up the machine and guaranteeing system reliability.

B. Related Research

The inductance detection strategies are more relevant to system design, system cost, and application situations. The position estimation methods are reviewed from the perspective of the way of inductance detection. The modulation method [6], [7], sensing coil method [7], [8], mutual inductance voltage method [9], [10], and the pulse injection method [10], [11], [13], [14] are typical inductance detection strategies. The modulation method occupies the idle phase as a part of the oscillation circuit, and a switching circuit is required to separate the drive circuit and detection circuit [6]. In the sensing coil method, the sensing coil is defined as a few turns of additional coils embedded into the stator slots for position estimation function. In this way, the inductance variation can be detected from the sensing coil instead of the armature windings [7], thereby no additional switching circuit is required. However, the stator slot is occupied by the sensing coil, and additional leads are introduced [8]. The mutual inductance voltage detection method can be applied in SRM with mutual inductance coupling between armature windings [9]. Also, this method can be applied to DF-DSM with mutual inductance coupling between field and armature windings [10]. Unfortunately, additional detection circuits and voltage sensors are required, thus increasing the system's cost and weight. By injecting pulses to detect self-inductance saliency, the pulse injection method is more friendly for initial position estimation as only current sensors are required [10], [11], [12], [13], [14], [20]. Similarly, by detecting the current slopes in one PWM cycle, initial position estimation is achieved in a minor saliency PM machine [15].

For accurate position estimation, compared with the method that requires premeasurements [12], the methods without premeasurements are more attractive. A Type-V exponential regression method is proposed in [16] but is easily influenced by modeling error. To tackle the inductance model mismatch, an

Manuscript received 6 July 2022; revised 27 August 2022 and 24 September 2022; accepted 11 October 2022. Date of publication 27 October 2022; date of current version 26 December 2022. This work was supported in part by the National Natural Science Foundation of China under Project 52077187 and in part by the Research Grant Council of the Hong Kong Government under Project PolyU 152143/18E and PolyU 152109/20E. (*Corresponding author: Shuangxia Niu.*)

Weiyu Wang and Shuangxia Niu are with the Department of Electrical Engineering, The Hong Kong Polytechnic University, Hung Hom, Hong Kong (e-mail: weiyu.wang@connect.polyu.hk; eesxniu@polyu.edu.hk).

Xing Zhao is with the Department of Electronic Engineering, University of York, YO10 5DD York, U.K. (e-mail: xing.zhao@york.ac.uk).

Color versions of one or more figures in this article are available at <https://doi.org/10.1109/TPEL.2022.3217576>.

Digital Object Identifier 10.1109/TPEL.2022.3217576

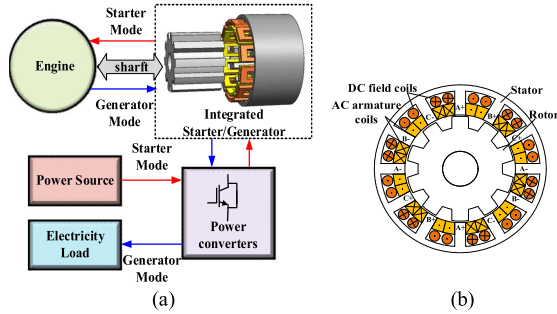


Fig. 1. ISG system. (a) Construction of system. (b) Structure of 12/10 DC-VRM.

optimized initial estimation method based on the finite element method is proposed to improve estimation accuracy [17]. Inductance geometric model methods such as the triangle model [10] are another effective strategy to acquire reliable position estimation without premeasurement and simulation.

C. Research Contributions and Implications

Although the studied DC-VRM has a doubly salient structure, the saliency in self-inductance is canceled out by winding connections [12], thus making the traditional self-inductance detection method inapplicable.

By analyzing the field and armature winding mutual inductance characteristics, a novel mutual inductance detection method for DC-VRM initial position estimation is proposed. The key is to integrate the sensing coil function into the field winding by operating the power transistor states, which means the field winding is reutilized as a sensing coil during the initial position estimation stage. Then, by injecting detection pulses into the armature windings, the induced currents in the closed sensing coil can be collected through current sensors.

The proposed method is designed for a group of nonsalient dc-excited machines with independent exciting fields and armature windings. It has good potential to be applied to a group of dc-excited machines such as DC-VRM, DF-DSM, hybrid-excited machines, and flux switching machines.

The proposed method is easy to implement and does not require additional detection circuits, embedded sensing coils, or voltage sensors at all. Therefore, it shows obvious advantages compared with the exiting modulation method, sensing coil method, and mutual induced voltage method. Combing the established series mutual inductance model, reliable initial position estimation can be achieved. The feasibility of the proposed method has been verified through theoretical analysis and experimental verification.

II. MACHINE STRUCTURE AND INDUCTANCES FOURIER CHARACTERISTICS

A. Configuration of 12/10 DC-VRM

The principle of ISG is illustrated in Fig. 1(a). The ISG can work as a starter to start up the engine and as a generator to transfer the energy from the engine to the electrical load. The structure of the 12/10 DC-VRM is provided in Fig. 1(b). Both dc and ac coils are wound on each stator tooth and two sets of

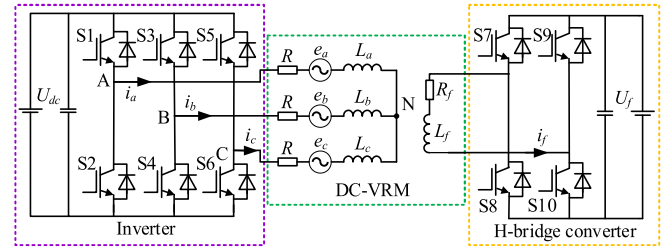


Fig. 2. Drive topology of 12/10 DC-VRM.

armature coils that have 180° phase differences are reversely cascaded to form a single-phase winding. The mathematical model and the parameters of the DC-VRM are presented in [4] and [12], respectively.

B. Self-inductance Characteristics

Fig. 2 presents the DC-VRM drive topology. Coil A+ is reversely connected with coil A- to constitute phase A. As coils A+ and A- have 180° phase differences, the Fourier expansion of their self-inductance L_{a+} and L_{a-} can be expressed as

$$L_{a+} = L_{adc} + \sum L_n \sin(n\omega t + \theta_n), n = 1, 2, 3 \dots \quad (1)$$

$$L_{a-} = L_{adc} + \sum L_n \sin(n\omega t + n\pi + \theta_n), n = 1, 2, 3 \dots \quad (2)$$

where L_{adc} is the dc component of self-inductance. L_n is the amplitude of the n th harmonics, ω is the electrical angular velocity, and θ_n is the initial phase angle of n th harmonics. The Fourier expansion of the self-inductance of phase A L_a can be regarded as the composition of coils A+ and A-.

$$\begin{aligned} L_a &= L_{a+} + L_{a-} \\ &= 2L_{adc} + 2 \sum L_n \sin(n\omega t + \theta_n), n = 2, 4, 6 \dots \end{aligned} \quad (3)$$

As shown in (3), the dc component is doubled while a saliency annihilation phenomenon occurs in L_a . The odd-order harmonics, including the fundamental component, are canceled when they are superimposed. As a doubly salient machine, the saliency effect mainly exists in the fundamental harmonic component. This phenomenon constrains the application of self-inductance saliency tracking sensorless drive methods.

C. Mutual Inductance Characteristics

For mutual inductance, M_{af+} and M_{af-} are the mutual inductance between field coils and the armature coils A+ and A-, respectively. Their Fourier expansion can be illustrated as

$$M_{af+} = M_{afdc} + \sum M_n \sin(n\omega t + \alpha_n), n = 1, 2, 3 \dots \quad (4)$$

$$M_{af-} = M_{afdc} + \sum M_n \sin(n\omega t + n\pi + \alpha_n), n = 1, 2, 3 \dots \quad (5)$$

where M_{afdc} is the dc component of mutual inductance. M_n is the amplitude of the n th harmonics, ω is the electrical angular velocity, α_n is the initial phase angle of n th harmonics. As coils

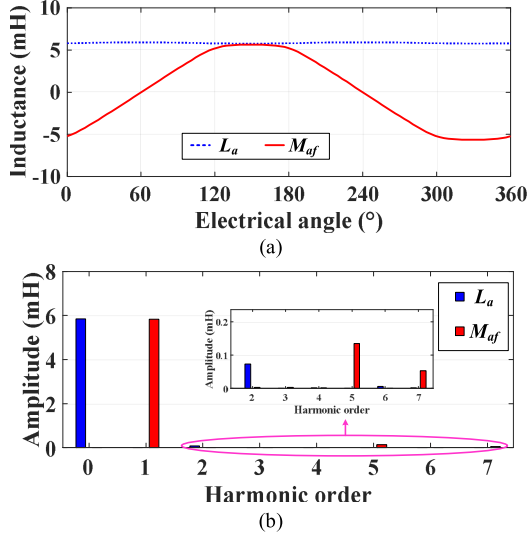


Fig. 3. Inductance of machine. (a) Self-inductance and mutual inductance. (b) Harmonics distributions.

A+ and A- have 180° phase difference, the Fourier expansion of the mutual inductance between phase A and the field coils is

$$\begin{aligned} M_{af} &= M_{af+} - M_{af-} \\ &= 2 \sum M_n \sin(n\omega t + \alpha_n), \quad n = 1, 3, 5, \dots \end{aligned} \quad (6)$$

It is clear to see from the final mutual inductance equation that the dc component and all the even-order harmonics are canceled, and all the odd-order harmonics, including the fundamental component, are doubled. Thence, position estimation can be designed based on mutual inductance characteristics. As seen in Fig. 3, the inductance characteristics have been verified through finite element analysis.

III. PROPOSED INITIAL POSITION ESTIMATION METHOD BY INTEGRATING SENSING COIL FUNCTION INTO FIELD WINDING

Based on mutual inductance characteristics, a novel initial position estimation method by integrating sensing coil function into field winding is proposed. By operating power transistor states, a closed sensing coil is acquired, and the detection signal is generated through the detection pulse in the armature winding. With the existence of mutual inductance coupling between the field winding and armature windings, an induced current can be detected in the closed sensing coil. Therefore, no additional detection circuits and voltage sensors are required, which means the drawbacks of the traditional embedded sensing coil method and mutual inductance voltage method can be overcome. In this way, the system cost can be further decreased, and system reliability can be guaranteed.

A. Pulse Injection Self-inductance Detection

As shown in Fig. 4, the detection pulse is injected into the field winding to detect the self-inductance of the field winding.

The equivalent voltage of field winding can be expressed as

$$U_f = L_f \frac{di_f}{dt} + i_f R_f \quad (7)$$

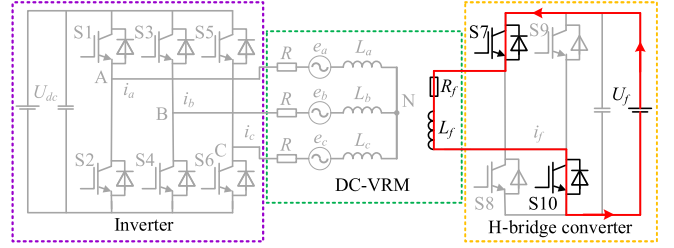


Fig. 4. Equivalent circuit of field winding pulse injection.

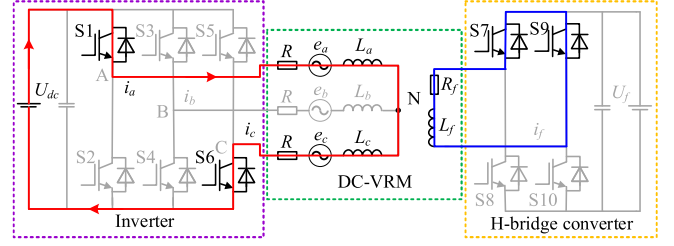


Fig. 5. Equivalent circuit of closed sensing coil and detection pulse injection.

where U_f is the dc voltage supply of the H-bridge converter, L_f is the self-inductance of the field winding, i_f is the resultant current of detection pulse, and R_f is the resistance of the field winding. As the detection pulsewidth is small, the resultant current is small, thereby the voltage drops of winding and power switches can be ignored [13]. L_f can be expressed as

$$L_f = \frac{U_f \Delta t}{I_f} \quad (8)$$

where Δt is the detection range that should be selected to avoid rotor moving and guarantee estimation accuracy [20]. I_f is the change value of the resultant current during the detection stage. Through the detection pulse method, the self-inductance of the field winding can be estimated.

B. Integrating Sensing Coil Method for Inductance Detection

As shown in Fig. 5, by switching on the power transistors S7 and S9, a closed sensing coil is achieved in the field winding. With the existence of mutual inductance coupling between field winding and armature winding, by injecting a detection pulse into the armature winding, an induced current can be detected from the established sensing coil. Therefore, the mutual inductance with the position information can be extracted.

The equivalent voltage equations of the established sensing coil and the series armature winding can be expressed as (9) and (10), respectively. The series mutual inductance M_{acf} can be expressed as (11).

$$U_{dc} = L_{a+c} \frac{di_a}{dt} + (M_{af} - M_{cf}) \frac{di_f}{dt} \quad (9)$$

$$0 = L_f \frac{di_f}{dt} + (M_{af} - M_{cf}) \frac{di_a}{dt} \quad (10)$$

$$M_{acf} = M_{af} - M_{cf} = \frac{-L_f \frac{I_f}{\Delta t}}{\frac{I_a}{\Delta t}} = \frac{-L_f I_f}{I_a} \quad (11)$$

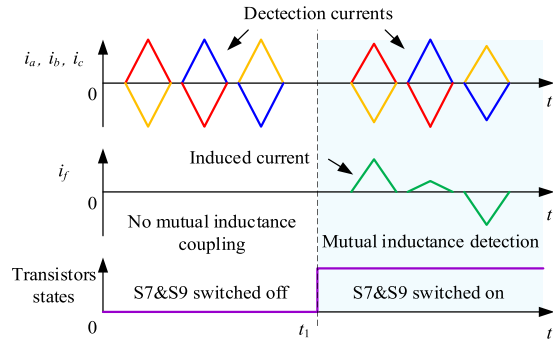


Fig. 6. Schematic diagram of the proposed mutual inductance detection method.

TABLE I
RELATION BETWEEN ELECTRICAL ANGLE, MUTUAL INDUCTANCES,
CONDUCTION PHASES, AND ROTOR SECTOR

θ ($^\circ$)	Inductance relation	Conduction phases	Sector
0–60	$M_{cbf} > M_{baf} > M_{acf}$	A and B	I
60–120	$M_{cbf} > M_{acf} > M_{baf}$	A and C	II
120–180	$M_{acf} > M_{cbf} > M_{baf}$	B and C	III
180–240	$M_{acf} > M_{baf} > M_{cbf}$	B and A	IV
240–300	$M_{baf} > M_{acf} > M_{cbf}$	C and A	V
300–360	$M_{baf} > M_{cbf} > M_{acf}$	C and B	VI

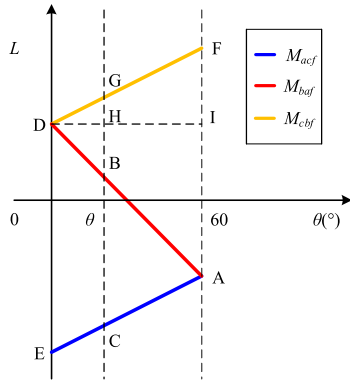


Fig. 7. Linearized series mutual inductance model in Sector I.

where I_a is the change value of the resultant current during the sampling stage. Similarly, by operating power transistor stages, the remaining mutual inductances M_{baf} and M_{cbf} between the armature windings and the field windings can be detected. To be more specific, the principle of the proposed method is illustrated in Fig. 6. Without a closed sensing coil in the field winding, when detection pulses are injected into the armature windings only, induced currents do not exist in the field winding. By switching on power transistors S7 and S9 from t_1 , a closed sensing coil is established, and its induced currents can be detected when detection pulses are injected into the armature windings. Then, by comparing the mutual inductance values, the initial position estimation can be estimated in Table I.

To estimate the initial electrical angle, the linearized mutual inductance model is established in sector I in Fig. 7. In the parallelogram DEAF in Fig. 7, triangles DBG and DAF are similar

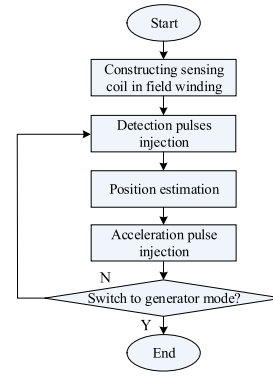


Fig. 8. Flowchart of position sensorless startup.

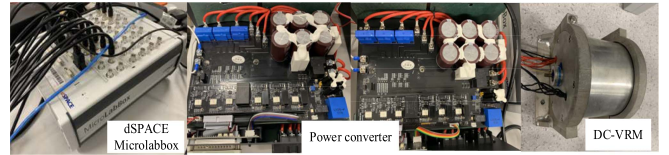


Fig. 9. Experimental setup of the proposed initial position estimation method.

triangles. Therefore, the following equation can be acquired.

$$\frac{\theta}{60^\circ} = \frac{DH}{DI} = \frac{GB}{FA} = \frac{GB}{GC} = \frac{M_{cbf} - M_{baf}}{M_{cbf} - M_{acf}} \quad (12)$$

Similarly, in the full electrical period, the initial position θ can be estimated as

$$\theta = \begin{cases} \frac{60^\circ (M_{cbf} - M_{baf})}{M_{cbf} - M_{acf}}, & \text{sector} = 1 \\ \frac{60^\circ (M_{acf} - M_{baf})}{M_{cbf} - M_{baf}} + 60^\circ, & \text{sector} = 2 \\ \frac{60^\circ (M_{acf} - M_{cbf})}{M_{acf} - M_{baf}} + 120^\circ, & \text{sector} = 3 \\ \frac{60^\circ (M_{baf} - M_{cbf})}{M_{acf} - M_{cbf}} + 180^\circ, & \text{sector} = 4 \\ \frac{60^\circ (M_{baf} - M_{acf})}{M_{baf} - M_{cbf}} + 240^\circ, & \text{sector} = 5 \\ \frac{60^\circ (M_{cbf} - M_{acf})}{M_{baf} - M_{acf}} + 300^\circ, & \text{sector} = 6 \end{cases} \quad (13)$$

The proposed position estimation method can be combined with the pulse injection method [10] to start up the machine. As shown in Fig. 8, the sensing coil is constructed in the field winding by operating power transistors, and then detection pulses are injected from the armature windings to detect the mutual inductance. Position estimation can be achieved through the established series mutual inductance model. Then the conduction phases can be decided, and the acceleration pulses are injected to drive the machine.

VI. EXPERIMENTAL RESULTS

As shown in Fig. 9, to verify the proposed method, the experiments are performed based on dSPACE MicroLabBox. A three-phase inverter and an H-bridge converter are applied for armature windings and the field winding, respectively.

The experimental results of constructing sensing coil initial position estimation are shown in Fig. 10. The detection pulses are injected into the armature windings, and the pulse width is 0.3 ms. By switching on power transistors S7 and S9, a closed

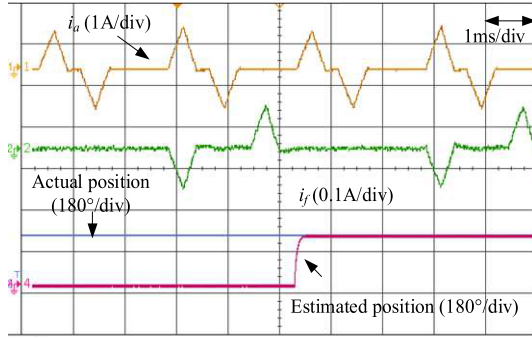


Fig. 10. Integrating sensing coil function for initial position estimation.

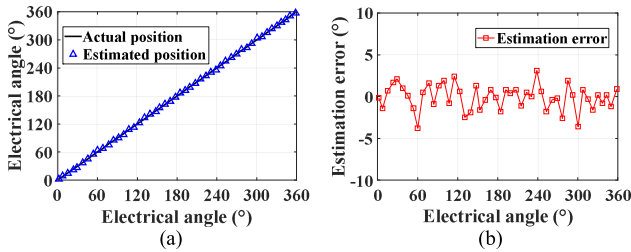


Fig. 11. Initial position estimation. (a) Actual position and estimated position. (b) Estimation error.

sensing coil is acquired in the field winding, then the resultant currents can be collected to calculate the mutual inductance and then calculate the initial position.

To verify the position estimation accuracy by the established mutual inductance model, the rotor is manually located in the different initial positions. In Fig. 11, the actual position and the estimated position are compared. An initial position estimation accurate to a 4° electrical angle corresponding to a 0.4° mechanical rotor angle can be achieved.

After the initial position estimation, the proposed position estimation method is combined with the pulse injection method to start up the machine. Detection pulses and acceleration pulses are injected into the armature windings sequentially to detect the rotor position and start up the machine, respectively. The field winding is operated as a current chopping mode, and the position information can be effectively acquired by the proposed method. A reliable position sensorless startup can be found in Fig. 12.

Not only for initial position estimation but the proposed method can also be applied during the free-running stage. As shown in Fig. 13, the detected mutual inductances are symmetrically distributed, and reliable position estimation can be achieved.

V. DISCUSSION AND CONCLUSION

This letter presents a novel initial position estimation method by integrating sensing coil function into field winding for nonsalient DC-VRM targeting aerospace high-reliability applications. The key is to operate the power transistor states to acquire a closed sensing coil in the field winding, and then detection pulses are injected into the armature windings to detect the mutual inductance. The mutual inductance model is established,

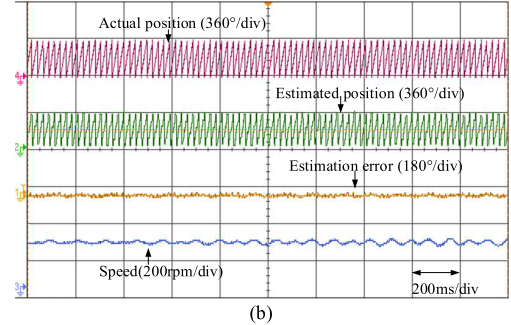
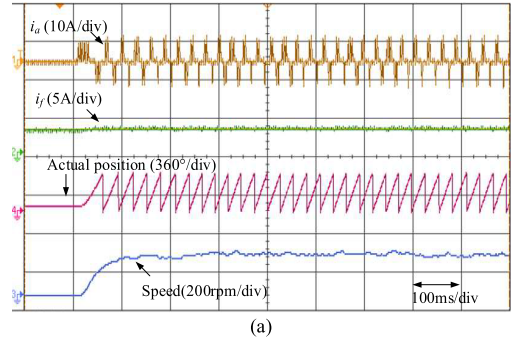


Fig. 12. Experimental results. (a) Position sensorless startup experiment. (b) Position estimation during the startup stage.

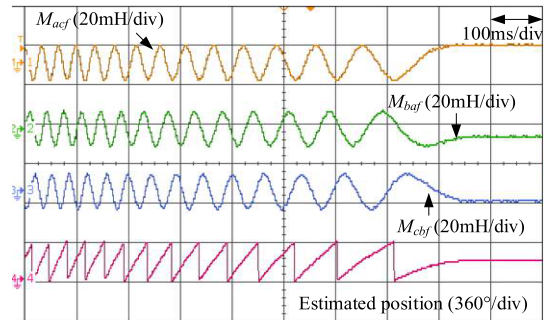


Fig. 13. Position estimation in a free-running stage.

and the initial position estimation error can be controlled within the range of 0.4° mechanical rotor angle. To guarantee position estimation accuracy, a high sampling rate is necessary, and the voltage delay caused by parasitic capacitance can be considered. It should be noted that the detection range is at a standstill and low-speed ranges. The back-EMF is increased with rotor speed. To achieve a full-speed sensorless drive and guarantee smooth transmission, high-speed sensorless drive methods should be combined [13], [18], [19], and the suitable detection range can be selected by experience, experiments, or trial-and-error methods [13], [19].

The proposed method is easy to implement, and additional detection circuits, embedded sensing coils, and terminal voltage sensors are not required. The proposed method is verified by experiments in the initial position estimation stage, startup stage, and free-running stage. Moreover, the proposed method can also provide reliable position estimation for the drive system with an incremental encoder to avoid the startup jitter and reverse.

REFERENCES

- [1] B. Sarlioglu and C. T. Morris, "More electric aircraft: Review, challenges, and opportunities for commercial transport aircraft," *IEEE Trans. Transp. Electric.*, vol. 1, no. 1, pp. 54–64, Jun. 2015.
- [2] Y. Jin, B. Bilgin, and A. Emadi, "An extended-speed low-ripple torque control of switched reluctance motor drives," *IEEE Trans. Power Electron.*, vol. 30, no. 3, pp. 1457–1470, Mar. 2015.
- [3] Z. Bian, Z. Zhang, and L. Yu, "Synchronous commutation control of doubly salient motor drive with adaptive angle optimization," *IEEE Trans. Power Electron.*, vol. 35, no. 6, pp. 70–81, Jun. 2020.
- [4] X. Liu and Z. Q. Zhu, "Stator rotor pole combinations and winding configurations of variable flux reluctance machines," *IEEE Trans. Ind. Appl.*, vol. 50, no. 6, pp. 3675–3684, Nov./Dec. 2014.
- [5] T.-W. Chun, Q.-V. Tran, H.-H. Lee, and H.-G. Kim, "Sensorless control of BLDC motor drive for an automotive fuel pump using a hysteresis comparator," *IEEE Trans. Power Electron.*, vol. 29, no. 3, pp. 1382–1391, Mar. 2014.
- [6] M. Ehsani, I. Husain, and A. B. Kulkarni, "Elimination of discrete position sensor and current sensor in switched reluctance motor drives," *IEEE Trans. Ind. Appl.*, vol. 28, no. 1, pp. 128–135, Jan.–Feb. 1992.
- [7] S. Rafael, P. J. Costa Branco, and A. J. Pires, "Srm sensorless for position control based on a frequency modulation system," *Meas.: J. Int. Meas. Confederation*, vol. 146, pp. 171–178, 2019.
- [8] J. Cai, Z. Liu, Y. Zeng, H. Jia, and Z. Deng, "A hybrid-harmonic-filter-based position estimation method for an SRM with embedded inductive sensing coils," *IEEE Trans. Power Electron.*, vol. 33, no. 12, pp. 10602–10610, Dec. 2018.
- [9] I. Husain and M. Ehsani, "Rotor position sensing in switched reluctance motor drives by measuring mutually induced voltages," *IEEE Trans. Ind. Appl.*, vol. 30, no. 3, pp. 665–672, May–Jun. 1994.
- [10] X. Zhou, B. Zhou, J. Yu, L. Yang, and Y. Yang, "Research on initial rotor position estimation and anti-reverse startup methods for DSEM," *IEEE Trans. Ind. Electron.*, vol. 64, no. 4, pp. 3297–3307, Apr. 2017.
- [11] M. Krishnamurthy, C. S. Edrington, and B. Fahimi, "Prediction of rotor position at standstill and rotating shaft conditions in switched reluctance machines," *IEEE Trans. Power Electron.*, vol. 21, no. 1, pp. 225–233, Jan. 2006.
- [12] W. Wang, X. Zhao, and S. Niu, "Predictive-pulse-injection-based dual-inverter complementary sensorless drive for 12/10 DC vernier reluctance machine," *IEEE Trans. Power Electron.*, vol. 37, no. 7, pp. 8369–8378, Jul. 2022.
- [13] E. Ofori, T. Husain, Y. Sozer, and I. Husain, "A pulse-injection-based sensorless position estimation method for a switched reluctance machine over a wide speed range," *IEEE Trans. Ind. Appl.*, vol. 51, no. 5, pp. 3867–3876, Sep./Oct. 2015.
- [14] W. Wang, X. Zhao, S. Niu, and W. Fu, "Comparative analysis and optimization of novel pulse injection sensorless drive methods for fault-tolerant DC vernier reluctance machine," *IEEE Trans. Power Electron.*, vol. 37, no. 11, pp. 13566–13576, Nov. 2022.
- [15] C. Wang and L. Xu, "A novel approach for sensorless control of PM machines down to zero speed without signal injection or special PWM technique," *IEEE Trans. Power Electron.*, vol. 19, no. 6, pp. 1601–1607, Nov. 2004.
- [16] Y. Chang, K. W. E. Cheng, and S. L. Ho, "Type-V exponential regression for online sensorless position estimation of switched reluctance motor," *IEEE/ASME Trans. Mechatronics*, vol. 20, no. 3, pp. 1351–1359, Jun. 2015.
- [17] L. Ge, H. Xu, Z. Guo, S. Song, and R. W. De Doncker, "An optimization-based initial position estimation method for switched reluctance machines," *IEEE Trans. Power Electron.*, vol. 36, no. 11, pp. 13285–13292, Nov. 2021.
- [18] L. Ge, J. Zhong, C. Bao, S. Song, and R. W. De Doncker, "Continuous rotor position estimation for SRM based on transformed unsaturated inductance characteristic," *IEEE Trans. Power Electron.*, vol. 37, no. 1, pp. 37–41, Jan. 2022.
- [19] A. Khalil et al., "Four-Quadrant pulse injection and sliding-mode-observer-based sensorless operation of a switched reluctance machine over entire speed range including zero speed," *IEEE Trans. Ind. Appl.*, vol. 43, no. 3, pp. 714–723, May–Jun. 2007.
- [20] J. Cai and Z. Deng, "Sensorless control of switched reluctance motor based on phase inductance vectors," *IEEE Trans. Power Electron.*, vol. 27, no. 7, pp. 3410–3423, Jul. 2012.